Available online at www.sciencedirect.com
SCIENCE DIRECT®

Journal of the European Ceramic Society 24 (2004) 3003–3011

www.elsevier.com/locate/jeurceramsoc

BST ceramics: Effect of attrition milling on dielectric properties

S. Tusseau-Nenez[a,b,*], J.-P. Ganne[a], M. Maglione[c], A. Morell[a], J.-C. Niepce[b], M. Paté[a]

[a]*THALES Research and Technology (TRT), Domaine de Corbeville, 91404 Orsay Cedex, France*
[b]*Université de Bourgogne, LRRS, UMR-CNRS 5613, BP47870, 21078 Dijon Cedex, France*
[c]*Institut de Chimie de la Matière Condensée de Bordeaux (ICMCB)—CNRS, 87 Av du docteur Albert Schweitzer, 33608 Pessac Cedex, France*

Received 21 November 2002; received in revised form 13 November 2003; accepted 21 November 2003

Abstract

The effect of grain size on the dielectric properties of $Ba_{0.6}Sr_{0.4}TiO_3$ (BST) ceramics is investigated. Attrition milling is chosen to obtain nanometre particle size from micrometre particle size powders. Fine grained ceramics are obtained by hot uniaxial pressing (HUP). Additionally, the present study is focused on the effect of the nature of milling balls on loss tangent and permittivity. For that, three kinds of balls are tested: calcia, yttria or ceria stabilised zirconia balls. The properties of these samples are evaluated in the range of MHz. The balls induce an involuntary doping of powders which modifies the dielectric properties, especially the Curie temperature and loss tangent.

Keywords: BST; (Ba, Sr) TiO_3; Dielectric properties; Grain size; Milling

1. Introduction

During the last decade, the effect of particle size on the dielectric properties of ferroelectrics has been investigated due to the great effort of miniaturisation of electronic devices. Various researchers studied the effect of grain size in ceramics of $BaTiO_3$, one of the well-known ferroelectric ceramics. It was established that the relative permittivity increases with the decrease of grain size down to 0.8 μm and then decreases with continuous grain size reduction.[1–8] The specific behaviour of the relative permittivity was explained according to several authors. Buessem et al.[1,2] supposed an increase of domain wall density with decreasing grain size. In small-grained ceramics (<1 μm), as the tetragonal distortion of the unit cell is smaller than in larger grained ceramics,[9] it is no more necessary to be compensated by formation of 90° domains. Martirena and Burfoot[3] proposed a model based on a Gaussian distribution of Curie temperatures T_C. Each grain has a different phase transition. The width of the Gaussian distribution increases when the grain size decreases. Finally, Arlt[5,6] proposed that the increase of the permittivity might be caused by the summation of domain size and stress effects. From the comparison of these studies with her own experiments, Valot et al.[10] concluded that no 90° domain wall can exist under 0.8 μm. The change in the domain microstructure may cause the change in permittivity versus grain size.[11]

The size reduction is also interesting for reducing the loss tangent. Actually, one knows that the motion of 90° domain walls is one of the sources of dielectric losses. In small-grained ceramics, the wall motion is limited by the pinning effect of grain boundaries,[8] which may reduce the value of loss tangent.

Moreover, in the last decade, some scientists studied the grain size effect on the dielectric properties at 100 kHz for the solid solution $Ba_xSr_{1-x}TiO_3$ (BST). For $x=0.3$, 0.5 and 0.7, Zhang et al.[12] showed that, as the grain size decreases, the transition temperature T_C and the relative permittivity decrease and the transition becomes diffuse. They concluded that, under grain sizes of 1 μm, the smaller grain size, the higher relaxation frequency.

For tunable devices, ceramics with a low to moderate permittivity and the lowest loss tangent are needed. Sengupta et al. showed the feasibility of such materials

* Corresponding author at present address. Centre d'Etudes de Chimie Métallurgique, UPR-CNRS 2801, 15 rue Georges Urbain, 94407 Vitry sur Seine, Cedex, France.
E-mail address: sandrine.nenez@glvt-cnrs.fr (S. Tusseau-Nenez).

0955-2219/$ - see front matter © 2003 Elsevier Ltd. All rights reserved.
doi:10.1016/j.jeurceramsoc.2003.11.019

by making composites of BST and various nonferroelectric oxides.[13,14] More recently, the authors studied the effect of milling composite powders on the optical[15] and microwave[16] properties of ceramics, but they give not much information on the correlation between microstructure and dielectric properties.

In the present study, $Ba_{0.6}Sr_{0.4}TiO_3$ was chosen because of its good combination of low T_C and relative low loss tangent. Ceramics with grain size under 0.8 μm were prepared in a similar way as already reported in $BaTiO_3$ ceramics.[17] The goal was to reduce the dielectric susceptibility and losses of BST because of the size effect. To achieve such sub-micrometre grain ceramics, attrition milling was chosen because it is an efficient process, easy to implement and to use on large scale batches.

The effects of various milling balls, calcia (ZrO_2–Ca), yttria (ZrO_2–Y) or ceria (ZrO_2–Ce) stabilised zirconia balls, on the milling efficiency are studied. The correlation between grain size and dielectric properties of BST ceramics is investigated. Finally, the dielectric properties of the ceramics are discussed.

2. Experimental procedure

$Ba_{0.6}Sr_{0.4}TiO_3$ micrometre powders are prepared by the solid-state method. Barium carbonate $BaCO_3$ (Merck 1711), strontium carbonate $SrCO_3$ (Prolabo 28311.297) and titanium dioxide TiO_2 (Toho 113), with the rutile structure, are milled together in water with yttria zirconia balls, diameter 12 mm, for 4 h in a Turbula® mill. The powders are dried in an oven at 120 °C. Then, the mixture is calcined at 1000 °C for 2 h in air.

The resulting powders are ground by attrition in water. In order to obtain the slurry, the calcined powder is ground in a mortar and milled together 4 h in water with yttria zirconia balls (diameter 12 mm) in a Turbula® mill. The obtained slurry is introduced in a laboratory attritor (Netzsch, type PR01S). During milling, the grain size reduction induces a thickening of the slurry. Therefore, to maintain the initial appearance, we added drop by drop an aqueous solution of Syntron (ammonium polymethacrylate) which is a dispersant. Three sorts of balls are used: ZrO_2–Y, perfectly spherical, ZrO_2–Ca or ZrO_2–Ce, which are rather spherical. The characteristics of the balls, given by the suppliers, are summed up in Table 1.[18,19] The resulting slurry is dried in a rotary evaporator. The rotating speed is fixed at 90 rpm/min and the temperature of the bath at 45 °C.

The phase identification is carried out by X-ray powder diffraction (SIEMENS, D5000 with $Cu_{k\beta}$ radiation) while the crystallite size is determined by the Williamson and Hall approximation. The morphology of the powders is observed by SEM and their mean grain size is calculated using the intercept line method on SEM micrographies. The densities are measured on the sintered samples via the geometric method, i.e. by weighing and measuring the dimensions of the sintered samples.

Fine-grained ceramics are prepared by hot uniaxial pressing (HUP) of the attrition-milled powders. First, the powder is pressed isostatically at 150 MPa. Samples are then sintered by HUP at 1100 °C, 1150 °C or 1200 °C for 1 h at 50 MPa. The heating rate is 50 °C.h^{-1} up to 500 °C to eliminate dispersants and then 100 °C.h^{-1}. After hot pressing, the sample is cooled down to ambient at 100 °C.h^{-1}. For comparison, conventional sintering (without pressure) is also implemented at higher temperatures (1300 °C and 1400 °C).

Relative permittivity and losses are measured from 10 kHz to 10 MHz, with a HP4194A impedance-metre. The Curie temperatures are determined at 100 kHz. The samples are pellets electroded with a high temperature silver paste screen-printed (10 mm diameter) on both faces and then heated at 700 °C for 25 min.

3. Attrition milling

3.1. Milling efficiency and grain size

Two significant parameters are taken into account: the evolution of the specific surface area, as a measure of the efficiency of grinding, and the type of the milling balls. For conditions 1 and 2, as a low concentrated aqueous Syntron solution is used, the resulting slurry is viscous. For conditions 3 and 4, a higher concentrated Syntron solution is used (Table 2). Even if less solution is added, because of the strong effect of Syntron (a drop modifies significantly the appearance of the slurry), the resulting slurry is fluid. Some other parameters are fixed (Table 3).

Fig. 1 shows the normalized specific surface area (S) versus milling time (t in hours). S is defined as $S = S_t/S_0$ where S_t is the specific surface area measured at time t

Table 1
Comparative typical properties and wear rate chart for zirconia milling beads

	Density	Diameter (mm)	Geometry	Life time (h)[a]	Wear loss (%)[a]	Colour
ZrO_2–Y	6.05	2 or 0.5 or 0.3	Spherical	3000	0.057	White
ZrO_2–Ca	5.4	≈1,5–2,4	Spheroid	<1500	>1.5	Sandy
ZrO_2–Ce	>6.1	1,7–2,4	Spheroid	3500	0.065	Brown

[a] After 15 h attrition milling, from technical reports.[18,19]

and S_0 the value of the powder before milling. The absolute values of the specific surface areas at $t=0$ h and $t=6$ h are given in Table 4. On Fig. 1, S increases continuously with milling time, showing the reduction of the particle size. After 6 h milling, S is about 10, 7.5 and 5.3 respectively for milling conditions 1, 2, 3 and 4.

In order to discuss the results obtained on similar slurry viscosities, the experiments corresponding respectively to the following milling conditions are compared:

- the milling conditions 1 and 2 for which the slurry seems very viscous,
- the milling conditions 3 and 4 for which for which the slurry seems fluider.

Table 2
Experimental milling conditions

Milling condition	Nature of balls	Mass of water (g)	Mass of syntron (g)
1	ZrO_2–Y	144	4.0
2	ZrO_2–Ca	125	5.2
3	ZrO_2–Y	110	6.9
4	ZrO_2–Ce	110	6.9

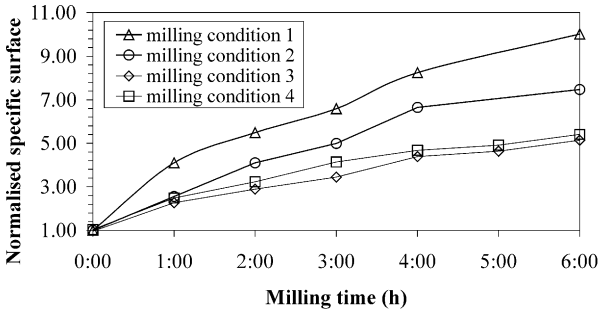

Fig. 1. Evolution of normalized specific surface area versus milling time for milling conditions 1, 2, 3 and 4.

Table 3
Experimental conditions fixed for all experiments

Powder weight in slurry (g)	Balls weight (g)	Milling time (h)	Speed of stirrer (rpm/min)
240	1400	6	500

It results that ZrO_2–Y balls are more efficient for grain size reduction than ZrO_2–Ca balls and that they are as efficient as ZrO_2–Ce balls. The quality of the geometry of balls is not a decisive factor for milling. Instead the density should be considered one of the most important characteristics to evaluate the milling performance of balls. The higher the specific gravity of the balls, the higher the milling efficiency.

The density of slurry is defined as the ratio of the powder mass to the water volume. For the milling conditions 3 and 4, the density was higher and the slurry contained more dispersant: the milling was less efficient. These results suggest that the use of dispersant must be controlled; an excess leading to a less milling efficiency.

The morphology and the grain size of powders after milling were observed by SEM (Fig. 2). Milling conditions 1 and 2 lead to powders with 220 nm average grain size whereas the powders obtained using milling conditions 3 and 4 have more spherical grains with 140 nm average particle size. In the latter case, the size distribution seems to be more uniform, probably due to a more homogeneous milling when the slurry is fluid.

The grains of powders obtained with milling conditions 1 and 2 are not spherical and exhibit rougher shapes (showing a drastic milling). Consequently, the estimate of the primary particle size, calculated with the approximation of spherical particles, gives an apparent smaller grain size compared to the grains of the powders milled using conditions 3 and 4. The grain size calculated from specific surface area, with this approximation, is smaller than the size of the primary grains, calculated from XRD analysis. The morphology of grains could explain this result.

SEM provides an estimate of the aggregates, the aggregates sizes are higher than those calculated with specific surface area values or XRD analysis. XRD gives information about the crystallographic domain size or crystallites. The calculations confirm that in milling conditions 3 and 4, the grain size reduction was more efficient.

In conclusion, even if the specific surface area is an important parameter to know, it must be completed by SEM and XRD measurements. Due to the good agreement between the grain size obtained using the specific surface area value and XRD analysis, it can be

Table 4
Comparison of specific surface areas and grain sizes obtained by SEM and XRD for different milling conditions

Milling condition (Table 2)	Specific surface area S_0 ($t=0$ h) ($m^2.g^{-1}$)	Specific surface area S ($t=6$ h) ($m^2.g^{-1}$)	Grain size (nm) specific surface area	Grain size (nm) SEM	Grain size (nm) XRD
1	1.4	14.1	76	220	145
2	2.0	15.2	70	220	240
3	2.4	12.9	82	140	85
4	2.6	13.5	78	140	85

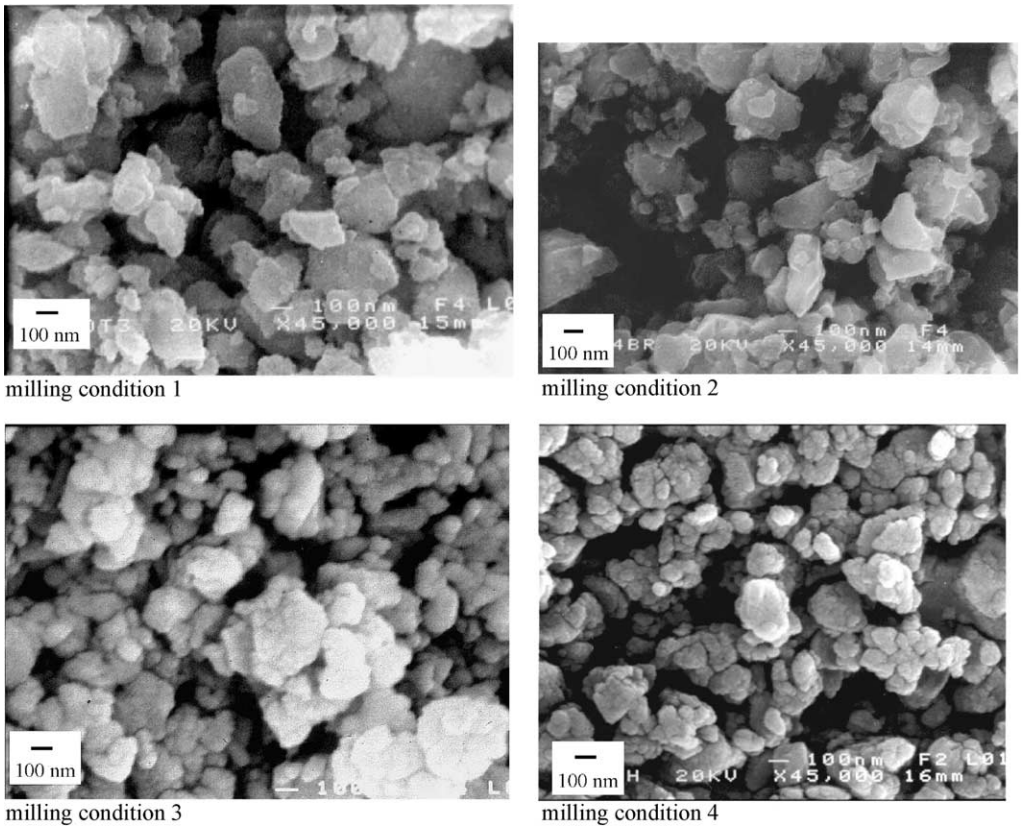

Fig. 2. Morphology of attrition-milled powders obtained with the different milling conditions.

concluded that the powders obtained with milling conditions 3 and 4 have a quite regular spherical shape about 85 nm in diameter and slightly aggregated.

3.2. Powder contamination

In Table 1, the wear loss of the balls is reported (technical reports by ball suppliers[18,19]). The data show that the pollution with ZrO_2–Ce balls is 14% higher than with ZrO_2–Y balls. The more polluting balls are ZrO_2–Ca, the less ones are ZrO_2–Y.

We wanted to check these wear loss values for ZrO_2–Y balls. For that, we weighed 100 new balls (i.e. never used) and 100 balls already used for about 500 h. Both weights were repeated four times (Table 5).

Table 5
Wear loss for the ZrO_2–Y balls before and after 500 h of milling

	Mass for 100 balls (g)	
Sample	New	Used (milling 500 h)
A	2.6949	2.6522
B	2.6853	2.6291
C	2.7052	2.6312
D	2.7002	2.6545
Average	2.6964	2.6417

Assuming that wear loss is proportional to milling time, we estimate its value to be about 0.004% after 1 h of milling and 0.062% after 15 h in order to compare with the technical reports. These results are in quite good agreement with those reported in the supplier data sheets (Table 1).

4. Ceramic sintering and microstructures

Conventional sintering and HUP were implemented and the corresponding dielectric properties were compared. All the results are summarised in Table 6.

For hot uniaxial pressing (HUP), as the sintering temperature increases, the grain size of the ceramics increases as it is shown on SEM micrographs (Fig. 3 a,b,c and Table 6). At 1100 °C, the relative densification d (78% of the theoretical density d_{th}) of ceramics occurs without any grain growth. Few grain boundaries are formed. At 1150 °C, the densification increases. Two areas appear: one is formed with 250 nm-sized grains and the second with formed and boundaried grains. At 1200 °C, the microstructure corresponds to a well densified ceramic (d=98% d_{th}), the grain size does not exceed 350 nm.

Fig. 3 (d,e,f) shows the microstructures of the ceramics obtained using powders obtained with different

Table 6
Density and average grain size of BST ceramics obtained by hot uniaxial pressing (HUP) and by conventional sintering

Milling conditions (reference to Table 2)	Sintering (temperature/duration/ atmosphere)	Nature of sintering	% of theoretical density [±1%]	Average grain size by SEM (nm) [±30 nm]
No milling	1300 °C/2 h/air	Conventional	89	650
Milling condition 1	1100 °C/1 h/air	HUP	78	185
	1150 °C/1 h/air	HUP	90	250
	1200 °C/1 h/air	HUP	99	350
	1300 °C/2 h/air	Conventional	92	10,000
	1400 °C/5 h/air	Conventional	96	30,000
Milling condition 2	1100 °C/1 h/air	HUP	80	130
	1200 °C/1 h/air	HUP	98	410
	1300 °C/2 h/air	Conventional	92	450 to 1700
	1400 °C/5 h/air	Conventional	90	2000 to 40,000
Milling condition 3	1200 °C/1 h/air	HUP	97	330
Milling condition 4	1200 °C/1 h/air	HUP	96	350
	1400 °C/5 h/air	Conventional	94	10,000

milling conditions and then conventionally sintered. Several factors influence the microstructure:

- the sintering temperature : the higher the sintering temperature, the larger the grain size. At 1400 °C/5 h/air, abnormal grain growth appears and limits the densification of the ceramic.
- the morphology of the powders: the abnormal grain growth is more important in case (e) than in case (f). In case (e), the powder exhibits grains with a rough form and a wide size distribution (corresponding to milling condition 2), two factors that promote abnormal grain growth. Conversely, in case (f), the grains are rounded and the grain size distribution seems to be regular.

5. Dielectric results

5.1. Curie temperature and grain size

In order to show the consequences of milling on the dielectric properties of fine-grained BST ceramics, the Curie temperatures were measured for different sintering conditions. The powders used were obtained with the milling condition 2. Fig. 4 (II is a zoom of I) shows the temperature dependence of the dielectric properties of BST ceramics at 1 MHz. It is important to notice the profile of the Curie peaks and their position. With decreasing grain size, the Curie peak becomes broader and less intense and tends to disappear. Moreover, the lower the grain size, the lower the Curie temperature. This behaviour was also noticed by Zhang et al.[12] for $Ba_xSr_{1-x}TiO_3$ ceramics ($x=0.3$, 0.5 and 0.7). Consequently, fine grain ceramics are interesting because of the limited change of the permittivity with temperature associated with the shifting of the Curie point to lower temperatures and a reduction of the amplitude of the Curie peak.

5.2. Curie temperature and type of balls

Fig. 5 shows the Curie peaks measured on ceramics obtained with no-milled powder and with attrition-milled powders (milling conditions 1 and 2). These ceramics were sintered conventionally at high temperature (1300 °C/2 h/air) in order to get large grain ceramics with well defined Curie peaks. The ceramic obtained with the no-milled powder exhibits a wide peak, centred at about −4 °C. When the powders are milled, the Curie peaks are narrower. A possible explanation is that milling could lead to a better chemical homogeneity of the powders and therefore to more uniform grain size of the ceramics. Chemical gradients in ceramics lead to a distribution of Curie temperatures and consequently to a broader peak.

When ZrO_2–Y balls are used, the peak is shifted towards higher temperature. In fact, Kell et al.[20] noted that, for $BaTiO_3$ ceramics, the substitution of Ti^{4+} ion by Zr^{4+} ion led to a reduction of the Curie temperature. Consequently, the observed shift of Curie point towards higher temperatures for our ceramics obtained using powders attrition-milled with ZrO_2–Y balls may be attributed to Y^{3+} ion. This behaviour was already observed with $BaTiO_3$ ceramics[21] and it is conceivable that the solid solution $BaTiO_3$–$SrTiO_3$ shows the same behaviour.

The Curie point is shifted towards lower temperatures under the combined effects of Zr^{4+} and Ca^{2+} ions.[22] Moreover, a reduction of the Curie temperature is observed.

Fig. 6 shows simultaneously the effect of milling balls and ceramic grain size on the Curie temperature. The major effect is due to the grain size: when grain size

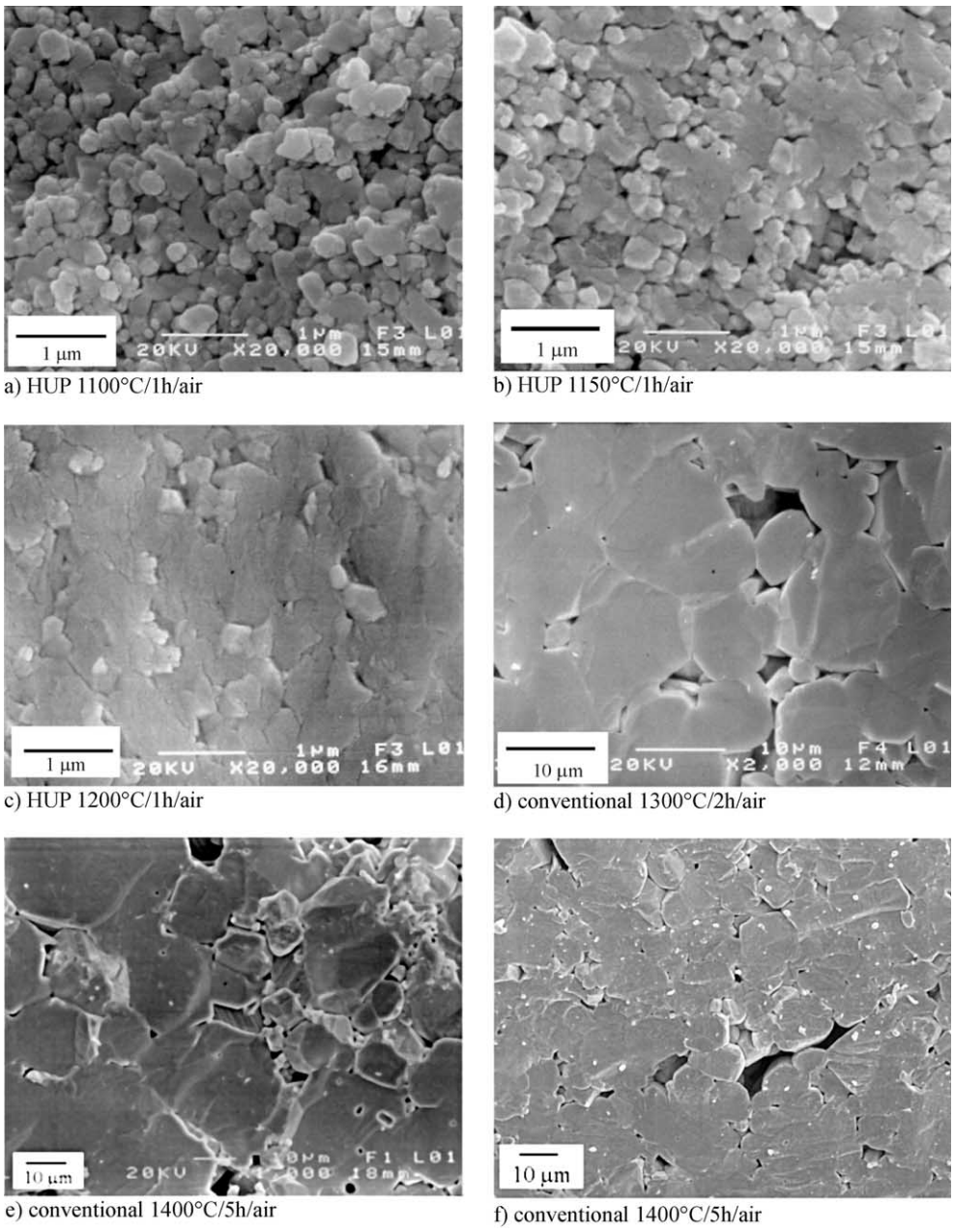

Fig. 3. Microstructures of $Ba_{0.6}Sr_{0.4}TiO_3$ ceramics obtained with ball-milled powders. (a) (b) (c) (d) correspond to milling condition 1, (e) milling condition 2 and (f) milling condition 4 (see Table 2).

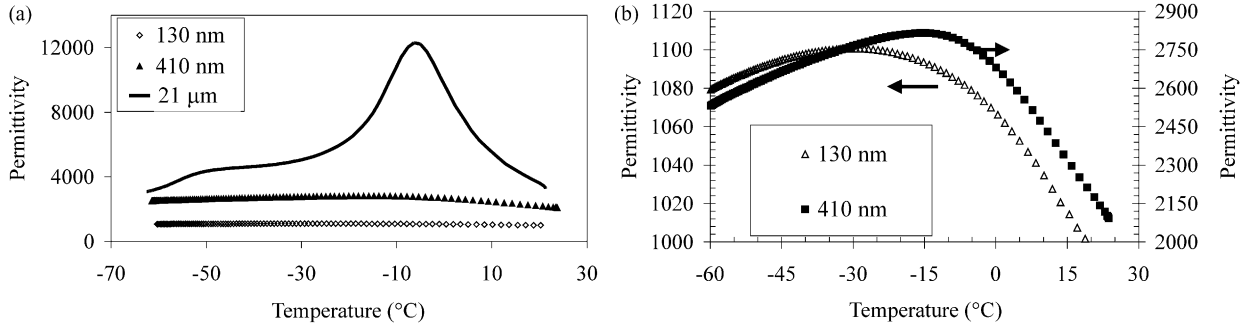

Fig. 4. Curie peak of $Ba_{0.6}Sr_{0.4}TiO_3$ ceramics for different grain sizes, at 100 kHz (II is a zoom of I). Powders are milled with ZrO_2–Ca balls and hot-pressed (130 or 410 nm-sized grains) or conventionally sintered (21 μm-sized grains) according to milling condition 2 (see Table 2 and Table 6).

decreases, the Curie temperature decreases. For the largest grain sizes, the Curie temperatures are higher when ZrO_2–Y balls are used. For small-grained ceramics, the effect of the type of balls is hidden by the reduction of the grain size.

We found that ZrO_2–Ce balls, which are as dense as ZrO_2–Y, give a milling efficiency as good as ZrO_2–Y (Fig. 3 and Table 6). Concerning the Curie temperature T_C, ZrO_2–Y balls and ZrO_2–Ce balls present opposite effects: milling with ZrO_2–Y balls increases T_C, while ZrO_2–Ce decreases T_C. The observed effect of ZrO_2–Ce balls is in agreement with the results of Yu et al.,[23] who noticed that, for the perovskite type $Ba(Ti_{1-x}Ce_x)O_3$ solid solutions, Ce doping shifts the maximum of permittivity to lower temperatures and gives dielectric properties more diffuse and dispersed.

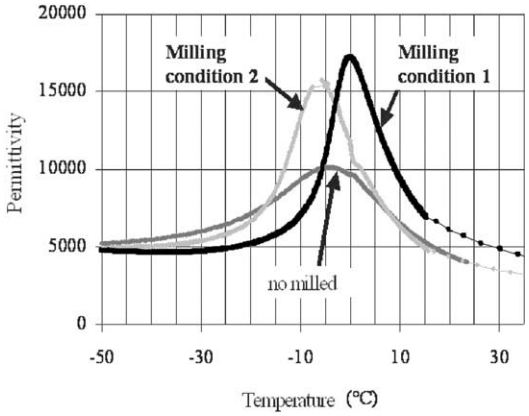

Fig. 5. Curie peak of $Ba_{0.6}Sr_{0.4}TiO_3$ large-grained ceramics at 100 kHz. Effect of milling conditions and type of balls: ZrO_2–Y for milling condition 1 and ZrO_2–Ca for milling condition 2. The powders are sintered at 1300 ° C/2 h/air.

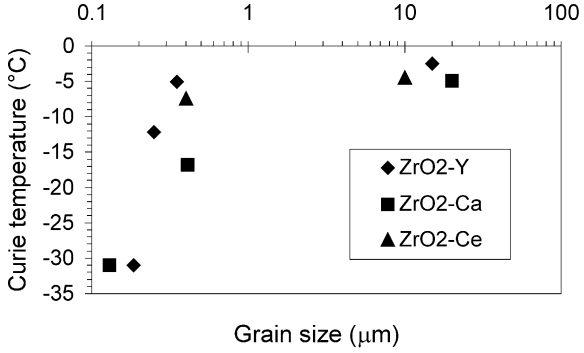

Fig. 6. Curie point of $Ba_{0.6}Sr_{0.4}TiO_3$ ceramics of different grain sizes obtained with attrition-milled powders with ZrO_2–Y (milling condition 1), ZrO_2–Ca (milling condition 2) or ZrO_2–Ce balls (milling condition 4).

5.3. Dielectric permittivities and losses

Table 7 presents the dielectric characteristics at 100 kHz as a function of temperature, measured on BST ceramics of different grain sizes. The powders used were attrition-milled with ZrO2–Ca balls. It is clearly shown that the dielectric characteristics depend on the grain size of the ceramics. As the grain size increases, the permittivity increases and the loss tangent decreases.

This behaviour is correlated with the Curie temperature, as already discussed in Section 5.1. As grain size decreases, the Curie temperature decreases and consequently the permittivity measured at the room temperature is lower. The peaks are more diffuse and their intensity decreases. In conclusion, small-grained ceramics have more stable dielectric properties with temperature. Moreover, the shift of the Curie peak according to the nature of the milling balls could explain why using ZrO_2–Ca and ZrO_2–Ce balls gives lower permittivities, as already discussed in Section 5.2.

Concerning the dielectric loss tangent, the grain size dependence is clearly shown. Large-grained ceramics exhibit the lowest dielectric loss tangent. The ceramics obtained by HUP have higher loss tangent whatever the sintering temperature. Those values of loss tangent could not be attributed to an effect of porosity because ϵ'' at 1100 and 1200 °C (respectively 77% and 98% of the relative density) are the same. The major effect seems to be attributed to the grain size because ceramics obtained by conventional sintering have better performances in spite of a residual porosity.

Table 8 gives the dielectric losses measured on ceramics sintered conventionally at 1400 °C/5h/air and therefore, showing large grain sizes. The results illustrate the effect of doping on BST powders.

Two cases are considered: (i) a voluntary doping, ie powders are doped with 1 mol% of Mn ($MnCO_3$ oxide is added to the raw materials), (ii) involuntary doping,

Table 7
Dielectric properties and grain size of ceramics obtained with attrition milled powders with ZrO_2–Ca balls (milling condition 2) at 100 kHz

Nature of sintering	Temperature/duration/atmosphere	Grain size (nm)	% Of theoretical density	ϵ'	ϵ''	tanδ (%)
HUP	1100 °C/1 h/air	130	77	1120	19.7	1.7
HUP	1150 °C/1 h/air	410	97	1880	33.0	1.8
HUP	1200 °C/1 h/air	465	98	3170	19.2	0.6
Conventional	1400 °C/5 h/air	1265	90	3150	4.1	0.09
Conventional	1465 °C/5 h/air	>10,000	92	4410	5.0	0.11

Table 8
Dielectric properties at 100 kHz of ceramics obtained from different attrition milled powders

Milling conditions (reference to Table 2)	Nature of sintering	Temperature/duration/ atmosphere	Nature of balls + voluntary doping	T_c (°C)	ϵ'	ϵ''	tanδ (%)
Milling condition 1	Conventional	1400 °C/5 h/air	ZrO_2–Y	−1	5160	12.0	0.2
Milling condition 2	Conventional	1400 °C/5 h/air	ZrO_2–Ca	−5	3150	4.1	0.1
Milling condition 3	Conventional	1400 °C/5 h/air	ZrO_2–Y + 1% mol Mn	−8	3554	6.6	0.2
Milling condition 4	Conventional	1400 °C/5 h/air	ZrO_2–Ce + 1% mol Mn	−11	3376	1.8	0.05

Table 9
Ionic radii (Å) and sites of substitution in $ABTiO_3$ type perovskite[24]

Site A		Site A or B	Site B								
Ba^{2+}	Sr^{2+}	Ca^{2+}	Bi^{3+}	Ti^{4+}	Mn^{3+}	Mn^{2+}	Ga^{3+}	Fe^{3+}	Y^{3+}	Nb^{3+}	Ce^{3+}
1.36	1.16	1.00	1.02	0.61	0.54	0.67	0.62	0.49	0.89	0.64	0.80

due to the pollution induced by the wear of the milling balls.

Firstly, the Mn-doping reduces the values of the Curie temperature. In consequences, ϵ' and ϵ'' are reduced. Nevertheless, tanδ is not modified. The kind of the milling balls has some effects on the dielectric properties. The shift of the Curie temperature leads to an increase of ϵ' and ϵ'' when ZrO_2–Y balls are used and a decrease when ZrO_2–Ca or ZrO_2–Ce balls are used.

Secondly, the effect of the valency of the dopant should be considered. Herner et al.[24] studied the effect of the doping of $Ba_{0.6}Sr_{0.4}TiO_3$ ceramics with Fe, Mn, Bi, Ga, Y, Nb, Ba and Sr. Following the example of Chiang and Takagi,[25] the ionic radii are summarised in Table 9. According to their value, they substitute in site A or B of the perovskite. Mn plays the role of acceptor: losses and permittivities are reduced, as Herner et al. showed. Y and Ce are donors. Usually, this doping leads to higher losses and permittivities. Combining Mn-doping and ZrO_2–Ce balls, tanδ is divided by 4.

6. Conclusions

This study shows that, compare to large-grained ceramics, attrition milling combined with hot uniaxial pressing (HUP) is interesting to obtain well densified ceramics ($d = 99\%$ dth) with fine grains (350 nm), with relative stable dielectric characteristics as a function of temperature. This is due to the shift of the Curie peak towards lower temperatures and to the reduction of the Curie peak amplitude. Nevertheless, the too high losses can not allow using fine-grained ceramics for the foreseen applications.

$Ba_{0.6}Sr_{0.4}TiO_3$ powders have been attrition-milled using three different kinds of balls which efficiencies have been compared. Ce and Y doped zirconia balls exhibit the best efficiency because of their density. ZrO_2–Ca balls are about 25% less efficient than the others. According to milling efficiency, ZrO_2–Ca should be excluded.

Large-grained ceramics have been obtained by conventional sintering of these powders. The effects of milling media on the dielectric characteristics have been studied. The Curie peak is shifted towards lower temperatures when ZrO_2–Ce and ZrO_2–Ca balls are used and the permittivities are reduced, because of the combined effects of doping the BST powders with Zr, Ca and Ce. When ZrO_2–Y balls are used, the Curie peak is shifted towards higher temperatures due to Y doping. A comparison of permittivity and loss tangent values shows that using ZrO_2–Ce gives lower values. A significant reduction of ϵ', ϵ'' and loss tangent has been successful with Mn doping.

Acknowledgements

The authors are grateful to thanks the Conseil Régional de Bourgogne who supported the S. Nenez thesis, this paper being part of the thesis.

References

1. Buessem, W., Cross, L. E. and Gosmani, A. K., Phenomenological theory of high permittivity in fine-grained barium titanate. *J. Am. Ceram. Soc.*, 1966, **49**, 33–35.
2. Buessem, W., Cross, L. E. and Gosmani, A. K., Effect of two-dimensional pressure on the permittivity of fine-and-coarse-grained barium titanate. *J. Am. Ceram. Soc.*, 1966, **49**, 36–39.
3. Martirena, H. T. and Burfoot, J. C., Grain-size effects on properties of some ferroelectric ceramics. *J. of Phys. C: Solid State Phys*, 1974, **7**, 3182–3192.

4. Kinoshita, K. and Yamaji, A., Grain-size effects on dielectric properties in barium titanate ceramics. *J. Appl. Phys.*, 1976, **47**, 371–373.
5. Arlt, G., Hennings, D. and With, G. D., Dielectric properties of fine-grained titanate ceramics. *J. of Appl. Phys*, 1985, **58**, 1619–1625.
6. Arlt, G., Böttger, U. and Witte, S., Emission of GHz shear waves by ferroelastic domain walls in ferroelectrics. *Appl. Phys. Lett.*, 1993, **63**, 602–604.
7. Bernaben, N., Leriche, A., Thierry, B., Niepce, J. C. and Waser, R., Pure barium titanate ceramics: crystalline structure and dielectric properties as a function of grain size. *Fourth Euro Ceramics*, 1995, **5**, 203–210.
8. McNeal, M. P., Jang, S.-J. and Newnham, R. E., Particle size dependent frequency dielectric properties of barium titanate. *J. of Appl. Phys*, 1996, **83**(6), 837–840.
9. Caboche, G., Berar, J. F., Mesnier, M. T., Niepce, J. C., Pannetier, J. and Ravet, M. F., Investigation indirecte des domaines ferroélectriques dans BaTiO3 à grains fins. *Silicates Industriels, Cer. Sci. Techn., T. LVIII*, 1993, **11-12**, 239–243.
10. Valot, C. M., Floquet, N., Perriat, P., Mesnier, M. and Niepce, J. C., Ferroelectric domains in BaTiO3 powders and ceramics evidenced by X-ray diffraction. *Ferroelectrics*, 1995, **172**, 235–241.
11. Niepce, J. C. *Diélectriques à grains très fins*, in Nanomatériaux, 2001, ARAGO n°27, under the leadership of H. VAN DAMME, OFTA Editor, Paris, p. 149–158.
12. Zhang, L., Zhong, W. L., Wang, C. L., Peng, Y. P. and Wang, Y. G., Size dependence of dielectric properties and structural metastability in ferroelectrics. *Eur. Phys. J. B*, 1999, **11**, 565–573.
13. Sengupta, L. C., Ngo, E., O'Day, M. E., Stowell, S. and Lancto, R., Fabrication and characterization of barium strontium titanate and non-ferroelectric oxide composites for use in phased array antennas and other electronic devices. *Proc. Inter. Symposium on Applications of Ferroelectrics*, 1994, 622–625.
14. Sengupta, L. C. Ceramic ferroelectric composite material-BST-magnesium based compound, US Patent 5,635,434, 1997.
15. Sengupta, L. C., Synowczynski, J. and Chiu, L. H., Investigation of the effect of particle size on the optical and electronic properties of Ba1-xSrxTiO3/MgO composite ceramics. *Integrated ferroelectrics*, 1997, **17**, 287–296.
16. Synowczynski, J., Sengupta, L. C. and Chiu, L. H., Investigation of the effect of particle size on the 10 GHz microwave properties of Ba1-xSrxTiO3/MgO composite ceramics. *Integrated ferroelectrics*, 1998, **22**, 341–352.
17. Perrot-Sipple, F., *Maîtrise de la taille de nanograins d'oxydes de structure pérovskite pour applications électrocéramiques : synthèse par chimie douce, broyage par attrition, Ph-D thesis*. University of Bourgogne, Dijon, France, 1999.
18. Jyoti Ceramics Indus, Technical Report, Alter Bahnhofsweg 1 D-49457 Drebber GERMANY.
19. Zircoa, Technical Report, Abraham Lincoln Strasse 1P.O. Box 2025 D-65010 Wiesbaden, Germany.
20. Kell, R. C. and Hellicar, N. J., Structural transformations in transformer materials of barium-titanate-zirconate. *Acustica*, 1956, **6**, 235–238.
21. Philips, N.V. Gloeilampenfabrieken, Ceramic dielectric, NL Patent n° NL 79706, 15 Nov. 1955.
22. Jules, J. C. *Défauts ponctuels par substitution et conséquences sur les transitions de phase et les propriétés diélectriques dans des composés du type A2BX4 et du type ABO3 (Ponctual defects obtained by substitution and effects on the phase transitions and the dielectric properties in compounds of type A2BX4 and type ABO3)*, PhD Thesis, University of Bourgogne, Dijon, France, 1989.
23. Yu, Z., Ang, C., Jing, Z., Vilarinho, P. M. and Baptista, J. L., Dielectric properties of Ba(Ti,Ce)O3 from 10e2 to 10e5 Hz in the temperature range 85-700 K. *J. Phys.: Condens. Mater.*, 1997, **9**, 3081–3088.
24. Herner, S. B., Selmi, F. A., Varadan, V. V. and Varadan, V. K., The effect of various dopants on the dielectric properties of barium strontium titanate. *Mat. Lett.*, 1993, **15**, 317–324.
25. Chiang, Y. M. and Takagi, T., Grain boundary chemistry of barium titanateand strontium titanate: II origin of electrical barriers in positive-temperature-coefficient thermistors. *J. Am. Ceram. Soc.*, 1990, **73**, 3286–3291.